

Processing Organic Waste Towards High Performance Carbon Electrodes for Electrochemical Capacitors

Krzysztof Wasinski^{1,*}, Piotr Nowicki², Paulina Pótrolniczak¹, Mariusz Walkowiak¹, Robert Pietrzak²

¹ Institute of Non-Ferrous Metals, Division in Poznań, Central Laboratory of Batteries and Cells, Forteczna 12, 61-362 Poznań, Poland

² Adam Mickiewicz University in Poznań, Faculty of Chemistry, Laboratory of Applied Chemistry, Umultowska 89b, 61-614 Poznań, Poland

*E-mail: krzysztof.wasinski@claio.poznan.pl

Received: 28 September 2016 / Accepted: 11 November 2016 / Published: 12 December 2016

Electrochemical properties of a family of carbons obtained from bio-waste have been investigated in terms of their application as electrode materials in electrochemical double layer capacitors. The precursor materials have been subjected to a special treatment involving activation in potassium carbonate and carbonization at 800°C in the flow of nitrogen. The resulting activated carbons exhibited high specific surface areas ranging from 840 to 1200 m² g⁻¹ and the total content of functional groups between 1.0 and 1.7 mmol per gram, depending on the source fruit material. Symmetrical capacitors have been assembled with two kinds of electrolytes, namely 6M KOH in water and 1M tetraethylammonium tetrafluoroborate in acetonitrile. Electrochemical characterization involved cyclic voltammetry, galvanostatic charge/discharge and electrochemical impedance spectroscopy techniques. Specific capacitances have been found to exceed 100 F g⁻¹ for 0.1 A g⁻¹ and to range from 17 to 45 F g⁻¹ for 10 A g⁻¹ in the aqueous electrolyte. In the organic electrolyte specific capacitances of 70 to 100 F g⁻¹ for 0.1 A g⁻¹ and 27 to 34 F g⁻¹ for 10 A g⁻¹ were determined. The observed high capacitances confirm that carbons obtained from waste biomass can be considered as promising electrode materials for high-performance supercapacitors.

Keywords: biowaste processing, one-step carbonization and activation, activated carbons, supercapacitors

1. INTRODUCTION

Electrochemical double later capacitors (EDLC) are widely regarded as a new promising type of electricity storage devices for applications requiring very fast charging and discharging as well as long service life of at least one hundred thousand cycles. In a typical configuration, an EDLC consists of two identical electrodes made of a high surface area carbon, with a separator in between, immersed

in either aqueous or organic electrolyte. The basic mechanism of electricity storage is based on the collection of electrical charges on both sides of each of the two electrode/electrolyte interfaces. When faradaic processes also take place during charge and discharge, the additional capacitance due to these reactions are referred to as pseudocapacitance. Very often, surface functional groups capable of undergoing redox reactions are responsible for the occurrence of pseudocapacitance. Since some charge transfer processes are virtually always present in addition to purely electrostatic phenomena, the terms pseudocapacitor, supercapacitor and ultracapacitor are widely used as synonyms of the term electrochemical double layer capacitor. The amount of stored charge is responsible for the observed capacitances of the electrodes as well as the cell as a whole. State-of-the-art EDLCs achieve gravimetric energy densities of 5 to 10 Wh kg⁻¹ and specific power of as much as 10 kW kg⁻¹ in addition to long cycle life, high safety level and no need of maintenance, making them the power source of choice for a growing set of applications, including electrical transportation [1-3].

Specific capacitance of an electrode material is proportional to its specific surface area, thus only materials having a very well developed pore structure can be considered as viable electrodes of EDLCs. In practice, only carbonaceous materials are used due to their high electronic conductivity, possibility of attaining extremely high surface areas, electrochemical and thermal stability, compatibility with polymeric binders, as well as relative facility of processing and low cost [4-7]. There have been enormous number of scientific works concerning synthesis, structure and electrochemical properties of carbon materials for electrochemical capacitors. Among studied types of carbons were activated carbons, carbon aerogels, carbon fibers, carbon nanotubes, graphene, and others [8-11].

Organic materials, including remains from plant processing, agriculture and forestry are a vast source of potential carbon precursors. Natural residues are abundant, inexpensive and their recycling contributes to conservation of natural environment. From chemical point of view they consist mostly of carbon-rich biopolymers such as celluloses, lignocelluloses, hemicelluloses, pectins, lignins, polysaccharides and proteins. This matter can be easily converted into carbonaceous materials by means of pyrolysis in an inert atmosphere. In addition, the resulting carbon structures can be tailored to any specific needs in terms of morphology, crystal structure, porosity and surface functionality by a wide range of well-established techniques, such as mild oxidation, chemical activation, template techniques, mechanical, chemical and thermal processing [12-14]. Activation of carbon materials can be accomplished by physical or chemical methods. The most common activation agent is KOH which produces micropores and increases pores width. ZnCl₂ was described as suitable agent for mesoporosity development whereas H₃PO₄ provides more heterogeneous pore size distribution. Recently, K₂CO₃ has become the activation agent of choice because of its non-toxicity, environmental friendliness and safety [15-17].

A significant number of biomass derived carbons have recently been proposed as electrode materials for EDLCs. Among precursors reported very recently have been coffee beans [18,19], banana skins [20] and fibers [21], tea leaves [22], willow catkins [23], sunflower seed shells [24], cassava skins [25], fibers of oil palm empty fruit bunches [26], and cherry stones [27]. Most of these carbons have been subjected to a certain activation procedure, such as that based on ZnCl₂ [18,19,21] or KOH [21-25,27]. Electrochemical capacitors with alkaline [20,22-24], neutral [21] acidic [18,25-27]

and organic [19,27] electrolytes have been assembled and tested electrically in these studies, resulting in capacitances ranging from 70 to 370 F g⁻¹ most often in three-electrode cells.

In the present work four new types of waste fruit skins have been selected and examined as precursors of carbon electrodes for EDLCs, namely originating from banana, grapefruit, mandarin and pomelo. Innovative chemical activation procedure has been applied to all the samples, giving rise to highly porous carbons. Application of potassium carbonate as activating agent allows to avoid heavy metal salts, corrosive acids or hydroxides, making the process environmentally benign.

2. EXPERIMENTAL

2.1 Preparation of activated carbons

The raw materials, waste skins of banana (BS), grapefruit (GS), mandarin (MS) and pomelo (PS) were first dried at 110°C and crushed down to the grain size of 2-4 mm. The materials were then impregnated with aqueous solution of potassium carbonate (99%, Aldrich) at the weight ratio 3:1 of K₂CO₃ to the carbon precursor, followed by drying to a constant mass at 110°C. This material was subsequently subjected to carbonization/activation step in nitrogen atmosphere (flow rate 330 mL min⁻¹). This process was carried out in a ceramic tubular reactor heated by a horizontal resistance furnace. The samples were heated at the rate of 10°C min⁻¹ from room temperature to 800°C, followed by annealing for 30 minutes and cooling down in nitrogen flow. After that the samples were rinsed with a hot 5% solution of hydrochloric acid and hot demineralized water. Finally, the samples were dried at 110°C. Activated carbons obtained from precursors BS, GS, MS and PS are designated as BSA, GSA, MSA and PSA, respectively.

2.2 Structural characterization

The elemental analysis of the raw precursors and activated carbons were performed using elemental analyzer CHNS Vario EL III (Elementar Analysensysteme GmbH). The ash content was determined according to the ISO 1171:2002 standard. Characterization of the pore structure of activated carbons was performed on the basis of low-temperature nitrogen adsorption-desorption isotherms measured with ASAP 2420 sorptometer (Micrometrics Instrument Corp.). Prior to the measurements the samples were outgassed at 300°C for 8 h. Surface area and pore size distribution were calculated using Brunauer–Emmett–Teller (BET) and Barrett–Joyner–Halenda (BJH) methods, respectively. Total pore volumes and average pore diameters were determined as well. Micropore volumes and micropore surface areas were calculated using t-plot method. To estimate the content of oxygen functional groups of acidic and basic character, the Boehm method was applied [28]. pH of the materials was evaluated using the procedure described in detail in our previous study [29].

2.3 Electrochemical characterization

The prepared carbons were mixed with polymeric binder (poly(vinylidene fluoride-co-hexafluoropropylene)), Kynar-Flex, Atofina) and acetylene black (C65, Timcal) at a mass ratio

80:15:5. Next, *N*-methylpyrrolidone (>99%, VWR) was added slowly. The obtained slurry was mixed for 2 h. The homogenic, viscous slurry was then cast onto stainless steel current collectors using the doctor blade technique. The prepared electrodes were vacuum dried at 105°C for 24 h. Symmetric two-electrode Swagelok-type cells with electrodes made of carbons BSA, GSA, MSA and PSA were assembled in argon filled glovebox (MBraun, H₂O < 0.5 ppm, O₂ < 0.5 ppm). Two electrolytes were used for studies: a) 6 M KOH (>99%, Aldrich) in distilled water and b) 1 M tetraethylammonium tetrafluoroborate ((C₂H₅)₄N⁺BF₄⁻, >99%, Aldrich) in acetonitrile (CH₃CN, >99.8%, Aldrich). Electrochemical experiments were performed with the application of multichannel potentiostat-galvanostat VMP-3 (Biologic). The following complementary techniques were applied: a) cycling voltammetry (CV) at scan rates from 1 to 200 mV s⁻¹, b) galvanostatic charge-discharge at current densities ranging from 0.1 to 10 Amperes per sum of masses of the two electrodes (A g⁻¹) and c) electrochemical impedance spectroscopy at the frequency range 100 kHz to 1 mHz and amplitude 10 mV.

Prior to the actual performance tests, maximum allowed operation voltages of supercapacitors were determined by CV technique. This was done by scanning for each carbon from the starting voltage of 0.0 V to a variable end-of-charge voltage ranging from 0.2 V to either 0.7 V (KOH) or 2.6 V (organics), with 0.1 V increments. The maximum operation voltage of a given capacitor was established as the last one at which a clear electrolyte decomposition peak could no longer be observed. Thus for subsequent experiments the maximum allowed voltages for 6 M KOH/water electrolyte based supercapacitors have been established as 0.6 V and for 1 M (C₂H₅)₄N⁺BF₄⁻ / CH₃CN electrolyte - as 2.5 V (with the exception of MSA for which 2.0 V has been found in organics). All specific capacitance values were calculated from Eqs. 1, 2 and 3 and have been expressed in farads per gram of active material per one electrode (F g⁻¹).

$$C = \frac{4 \int I(V) dV}{v(m^- + m^+) \Delta V} \quad \text{Eq. 1}$$

$$C = \frac{-4}{2\pi f Z_{img} (m^- + m^+)} \quad \text{Eq. 2}$$

$$C = \frac{4It}{U(m^- + m^+)} \quad \text{Eq. 3}$$

where:

C – specific capacitance for tested material recalculated for one electrode

ΔV – potential window of scanning

v – scan rate

f – frequency

Z_{img} – imaginary part of impedance

I – current

t – time of discharge

U – discharge voltage excluding the IR drop on start of discharge

m^- and m^+ – mass of negative and positive electrode material

3. RESULTS AND DISCUSSION

3.1 Chemical and structural characterization of carbons

Fig. 1 presents the results of ash content and elemental composition determined for the four carbon materials obtained by carbonization and activation of waste fruit skins. It can be seen that chemical activation with the application of potassium carbonate leads to activated carbons characterized by a very low mineral matter content, ranging from 1.0 to 2.1 wt. %. This is a very advantageous feature, especially from the electrochemical point of view, because this way inactive ballast is avoided. Low ash content results from the fact that substantial part of mineral matter present in raw materials has been decomposed in reaction with the activating agent (K_2CO_3) during heat treatment as well as subsequent washing of post-activation products with hydrochloric acid. Moreover, each carbon material is characterized by a very large content of elemental carbon (from 83.1 to 90.2 wt. %) and a relatively low content of heteroatoms, out of which the main part constitutes oxygen (ca. 10 wt. %). Important oxygen content can be attributed to a relatively low carbonization temperature, preserving large part of oxygen containing chemical groups abundant in the raw organic substance. It is noteworthy that surface oxygen functional groups, such as hydroxyl, carboxyl, ether, ester and, especially, quinone, can in fact be advantageous in terms of the application in electrochemical capacitors, being a possible source of pseudocapacitance [10,30].

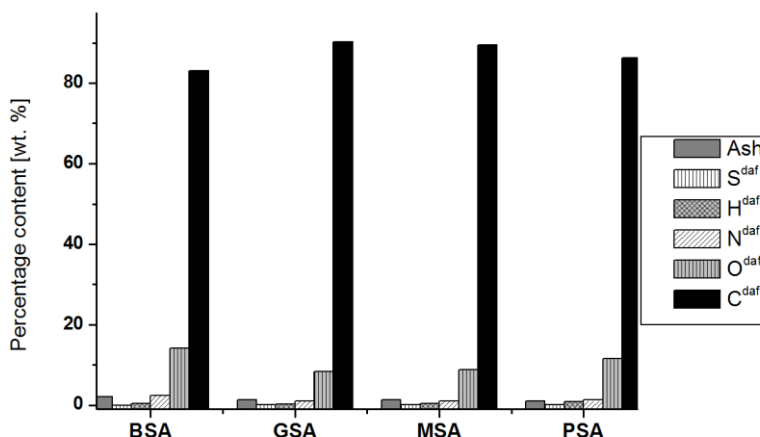


Figure 1. Ash content and elemental composition of the prepared activated carbons; ^{daf} - dry, ash-free basis, * - determined by difference).

Pore structure and volume is a factor of decisive importance for the efficiency of carbon based electrochemical capacitors. As follows from the data collected in Fig. 2, potassium carbonate can be considered as a very effective pore forming agent. The total surface area of the prepared materials ranges from $840 \text{ m}^2 \text{ g}^{-1}$ for PSA to $1200 \text{ m}^2 \text{ g}^{-1}$ in the case of GSA sample, whereas pore volume is within the range from 0.45 to $0.66 \text{ cm}^3 \text{ g}^{-1}$. Textural parameters of the investigated materials depend to a large extent on the type of precursor used for their preparation. This effect is very pronounced in the case of PSA sample, which exhibits significantly less favorable characteristics than the other activated carbons. Irrespective of the kind of precursor used, all materials show microporous character of the structure, as evidenced by the fact that the contribution of micropores in the total pore volume exceeds

60 %. The average pore diameter varies between 2.14 and 2.19 nm, thus the distribution is very narrow.

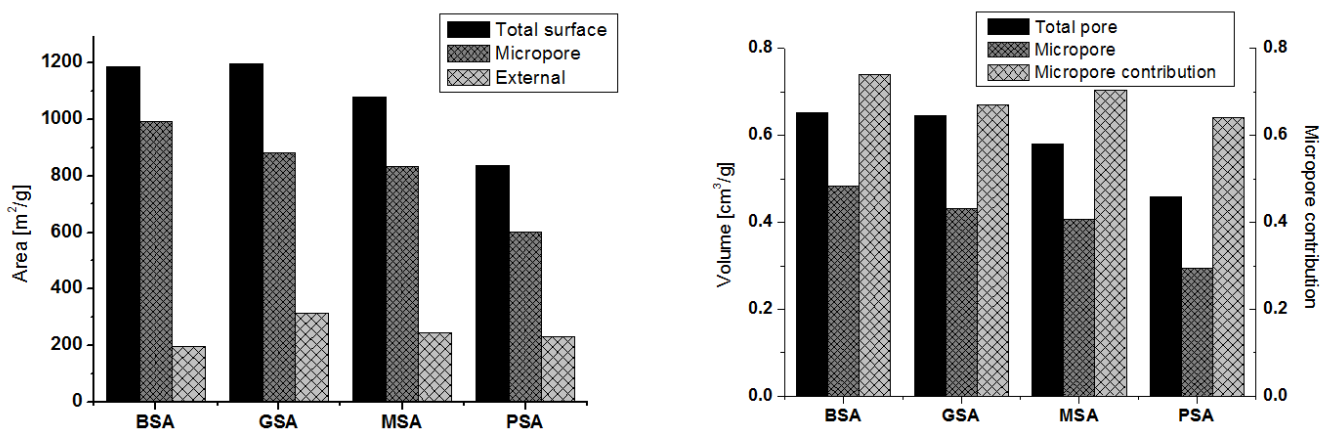


Figure 2. Textural parameters of the prepared activated carbons.

Based on data shown in the Fig. 3 it can be stated that the chemical activation of fruit skins with potassium carbonate leads to carbons with intermediate acid-base nature of the surface. Despite of the fact that each of the carbons has much more acidic groups than basic ones, their pH oscillates around the value of 7, suggesting that these groups are only weakly acidic. Acid-base properties of an activated carbon surface (similarly to textural parameters) depend on the type of precursor used for their preparation. The greatest content of acidic groups (1.44 mmol g^{-1}) is observed for PSA sample obtained from pomelo skin, while the greatest amount of functional groups of basic character (0.49 mmol g^{-1}) is present on the surface of BSA sample, prepared from banana skins.

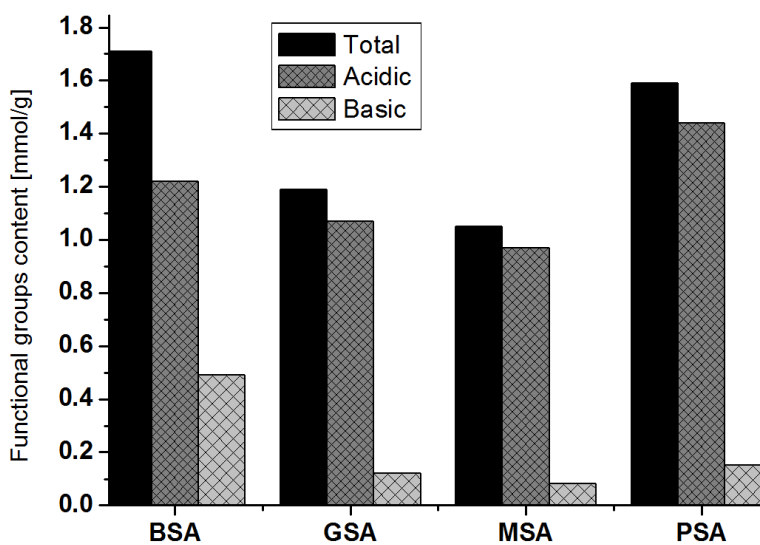


Figure 3. Acid-base properties of the prepared activated carbons.

3.2 Application of the prepared carbons as electrode material for EDLC

Aqueous and organic are the two most important classes of electrolytes for EDLCs. This fundamental division is based on the accessible voltage window of the device operation resulting from intrinsic electrochemical stabilities of organic and water based media. Cyclic voltammetry (CV), electrochemical galvanostatic charge-discharge and electrochemical impedance spectroscopy (EIS) techniques have been applied to determine specific capacitances at a range of load conditions.

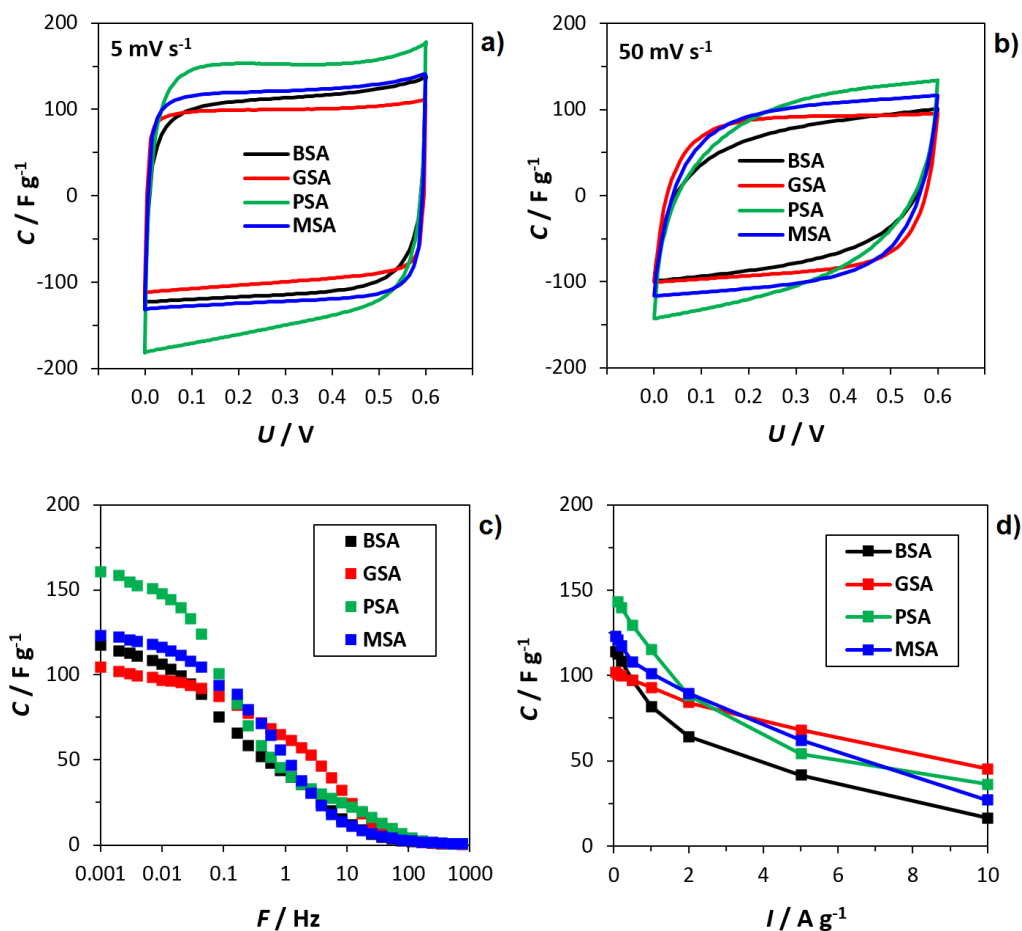


Figure 4. Cycling voltammetry, electrochemical impedance spectrum and capacitance vs. discharging current graph recorded for EDLC`s filled by 6 M KOH / H₂O electrolyte.

6 M water solution of KOH has been chosen as the aqueous electrolyte. Maximum voltage of the test cells has been set as 0.6 V in order to prevent water electrolysis and electrode materials degradation. Typical CV characteristics are presented in Figs 4a) and b). CV experiments not only allow for the determination of specific capacitances (numerical values are collected in Table 1; the capacitance calculations in symmetrical double layer capacitors have been based on Equations 1, 2 and 3 as well as in the works [8,31]) but also to assess the charge propagation phenomena on the basis of the curves shapes. As can be seen from Table 1, for the low scan rates of 1 to 5 mV s⁻¹ the discharge specific capacitances achieve 82 F g⁻¹ or more for all carbons. The highest value (more than 140 F g⁻¹)

was recorded for PSA sample. For moderate scan rates of 10 mV s⁻¹ to 50 mV s⁻¹ specific capacitances are in range from 65 to 131 F g⁻¹. At a fast scan rate of 200 mV s⁻¹ the specific capacitances were found to range from 34 F g⁻¹ to 46 F g⁻¹ depending on the sample. The CV curves feature near-rectangular shape typical for symmetric EDLC's. No distortions, peaks or waves are observed. The best charge propagation is represented by GSA also at high scan rates. BSA carbon represented resistance-type shape at 50 mV s⁻¹. PSA exhibits the highest capacitances of all carbons, especially at low scan rates.

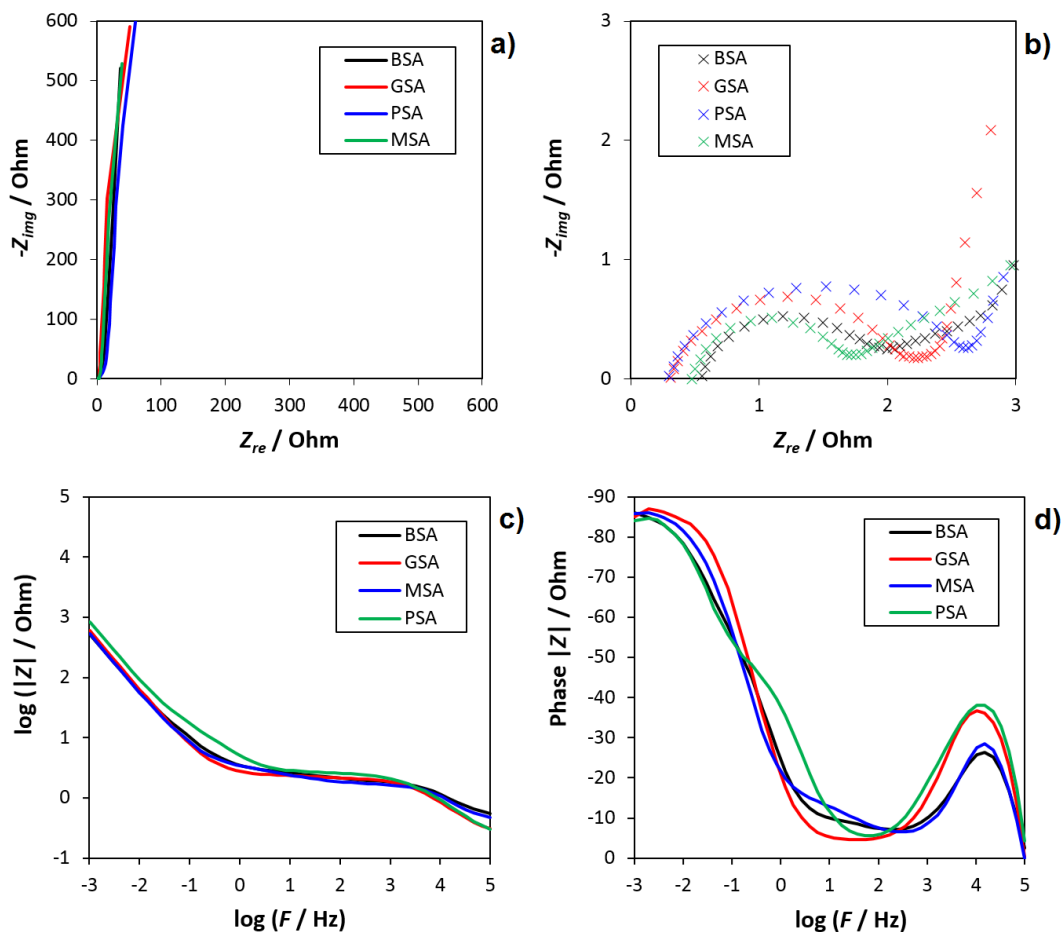


Figure 5. Nyquist plots and Bode plot for tested EDLC's filled by 6M KOH in H₂O.

The electrochemical impedance spectroscopy are shown in Fig.4c). and in Fig. 5. At the lowest frequency (1 mHz) the specific capacitances were higher than 100 F g⁻¹ for all carbons. The maximum capacitance of 158 F g⁻¹ was confirmed for PSA. Until 0.2 Hz PSA outperforms the other carbons. Interestingly, GSA, which somewhat lags behind at the lowest frequencies, at medium frequency range of 0.1 to 10 Hz appears to excel. Capacities recorded above 10 Hz are negligible but this is comprehensible for such a high rates. The Nyquist plots are presented in the Fig. 5 a) and b) and feature typical for EDLC's behavior with low Ohmic impedance. Small semi-circles in the high frequency regions correspond to low equivalent series resistance (ESR) and a very high parallel resistance connected with the double layer capacitance (DLC). The DLC values expressed as specific

capacitance for tested electrode materials were calculated from imaginary part of impedance (imaginary component, Z_{img}) and placed in Table 2. On the Bode plot (see Fig. 5 c) and d)) the phase angles at low frequencies were nearly -85° but could not reach -90° . This plot indicated predominant DLC of tested devices with typical high porous electrode materials.

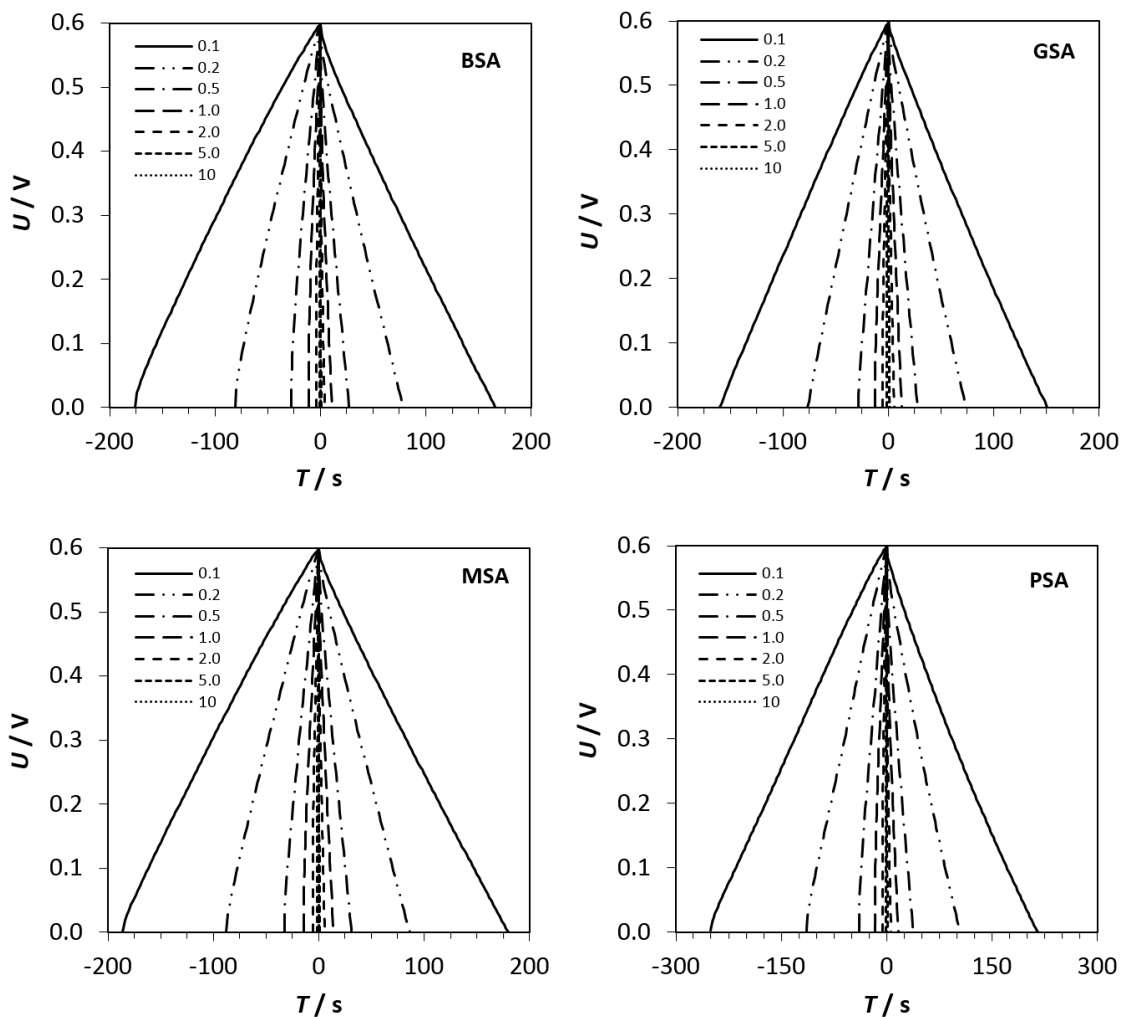


Figure 6. The galvanostatic charging-discharging profiles for EDLC`s filled by 6M KOH in H₂O recorded at 0.1 to 10 A g⁻¹.

The galvanostatic charge-discharge tests have been carried out at current loads from 0.1 to 10 A g⁻¹. The obtained capacitance data for all carbon samples have been represented in function of the current densities in the Fig. 4d). Generally, specific capacitances decrease with increasing current density which is in agreement with literature data [3, 32]. At 0.1 A g⁻¹ PSA exhibits the highest capacity of 143 F g⁻¹ and GSA – the lowest (101 F g⁻¹). However at the other end of the scale (10 A g⁻¹) GSA is the best with 45 F g⁻¹, which is still a significant output at this extreme current load. BSA retains the smallest capacitance at this point with only 17 F g⁻¹. The cell voltage versus time plots (see Fig. 6.) recorded for all capacitors were represented by typical triangular response for constant current charging and discharging. Sharp peaks with short time on this plots were observed at the highest

current rates such as 5 or 10 A g⁻¹. All capacitance values obtained and calculated from this technique were placed in Table 3.

1 M tetraethylammonium tetrafluoroborate solution in acetonitrile has been applied as the organic electrolyte. Selected electrochemical characteristics recorded for capacitors with this electrolyte are presented in Fig. 7. As far as cyclic voltammetry experiments are considered, BSA, GSA and PSA carbons have been cycled between 0 and 2.4 V whereas MSA has been tested between 0 and 2.0 V in order to avoid excessive electrolyte decomposition. Determination of the appropriate potential window has been carried out in a separate experiment prior to the studies discussed here (please refer to Experimental section for details). The CV curves recorded at 5 and 50 mV s⁻¹ (see Fig. 7a) and 7b), respectively) suggest that charge propagation is the best for MSA carbon, since its CV shapes approach rectangular shape most closely. However the differences between materials are not very pronounced. Table 1. collects capacitance data obtained from CV experiments at increasing scan rates. As can be seen, the calculated specific capacitances were in the range from 77 to 102 F g⁻¹ at low scan rates. The highest discharge specific capacitance of 102 F g⁻¹ was found for BSA sample. Specific capacitances at 50 mV s⁻¹ were found to be 60 F g⁻¹ for MSA and PSA, 63 F g⁻¹ for GSA and 68 F g⁻¹ for BSA and these value decreased to ca. 40 F g⁻¹ for all samples at 200 mV s⁻¹ scan rate.

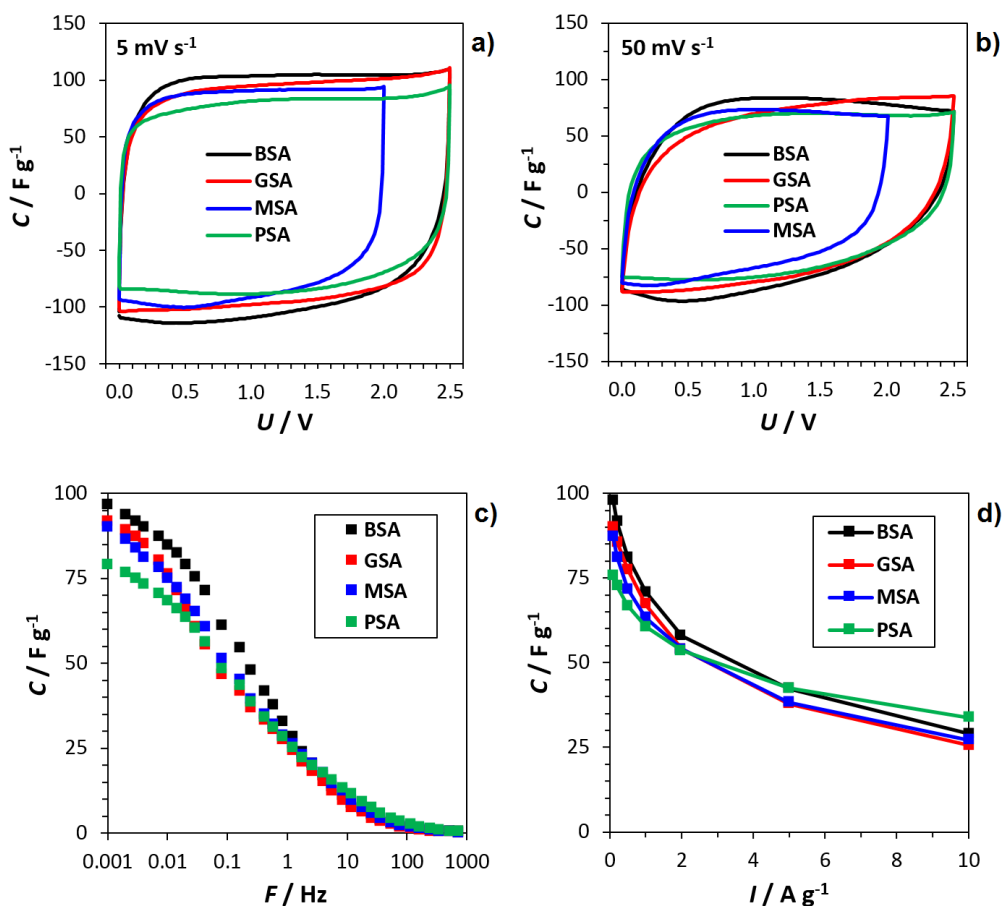


Figure 7. Cycling voltammetry, electrochemical impedance spectrum and capacitance vs. discharging current graph recorded for EDLC's filled by 1 M (C₂H₅)₄N⁺BF₄⁻ / CH₃CN electrolyte.

The capacitance vs. frequency plot is presented in the Fig. 7c). In the low frequency region (1 mHz) the specific capacitances are in the range from 80 to 97 F g⁻¹ and, similarly to what was observed for the aqueous electrolyte, they decrease rapidly with increasing frequency. At 1 Hz the capacitances reach ca. half of the values observed for the aqueous electrolyte, which can be obviously attributed to slower electrode kinetics, being an obvious feature of organic media. Interestingly, PSA performs the worst at slow rates, which is just the contrary to what was observed for the aqueous electrolyte. More detailed data with specific capacitance values and the corresponding frequencies were placed in Table 2. Nyquist plots on Fig. 8 a) and b) showed low ESR and low equivalent distributed resistance for EDLC's filled by organic electrolyte. In comparison Ohmic resistance were highest than for water electrolyte due to higher conductivity of this electrolyte. The Bode plot (Fig. 8 c) and d)) showed typical impedance and negative phase shift behavior vs. frequencies in low frequency region. At the highest frequencies specific hump were observed which is typical for EDLC's materials.

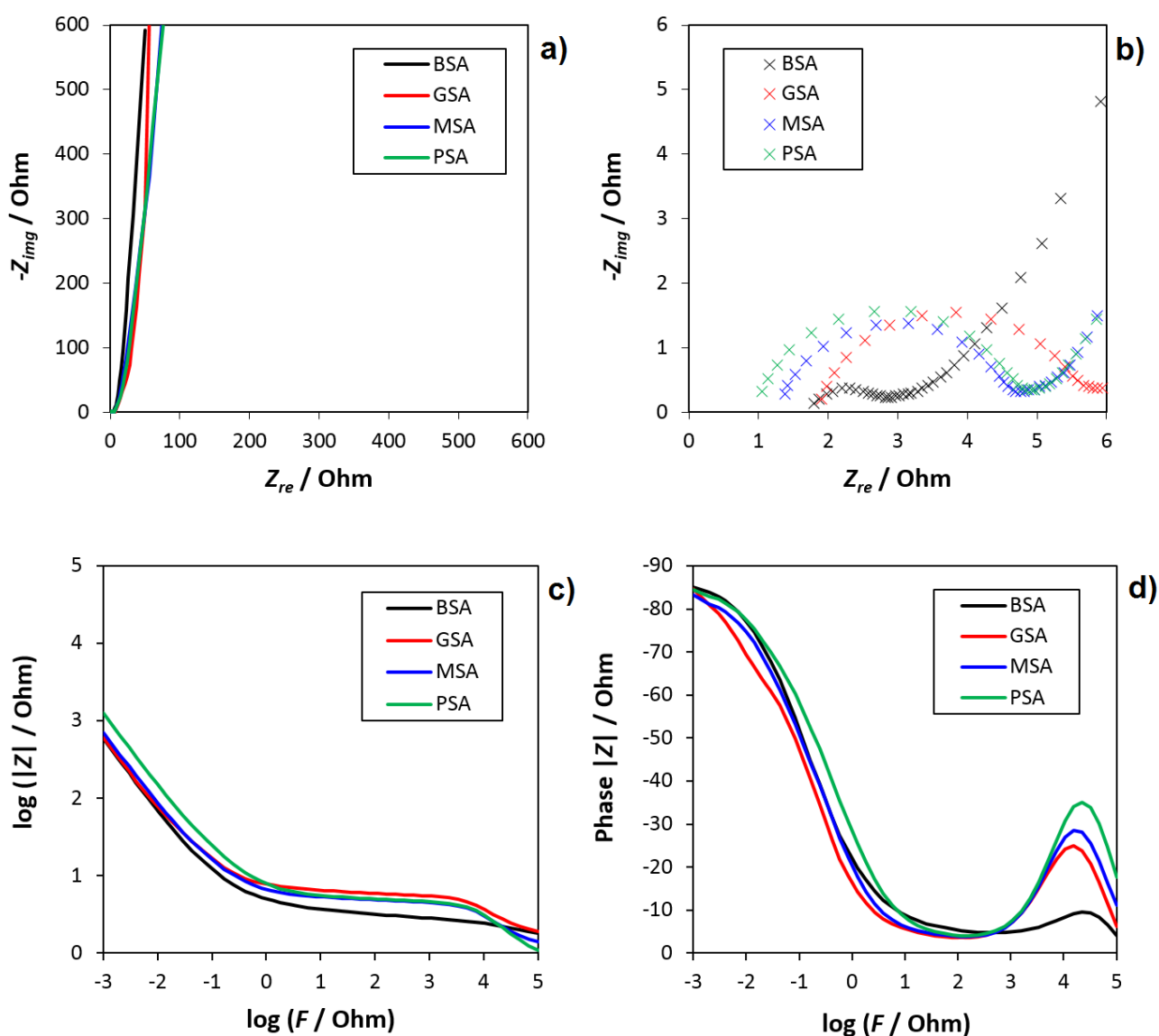


Figure 8. Nyquist plots and Bode plot for tested EDLC's filled by 1M (C₂H₅)₄N⁺BF₄⁻ in CH₃CN.

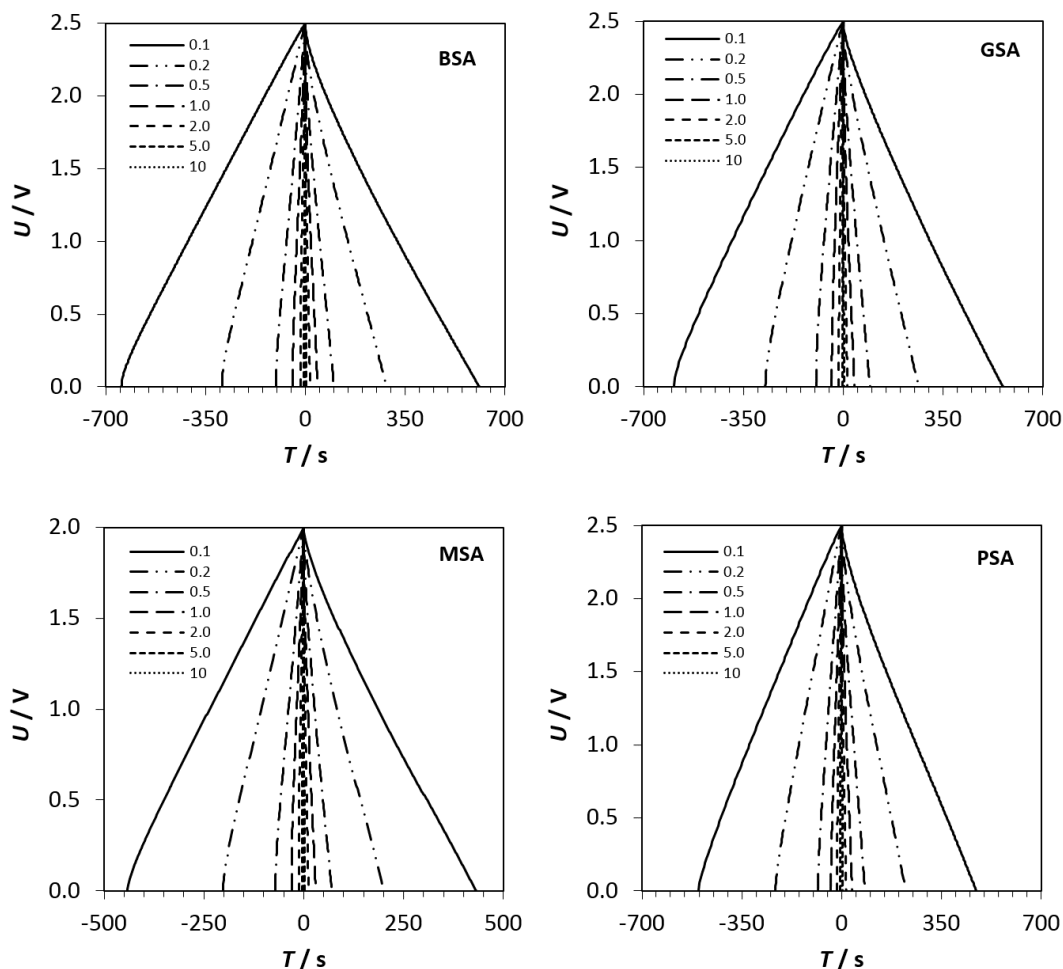


Figure 9. The galvanostatic charging-discharging profiles for EDLC`s filled by 1M (C₂H₅)₄N⁺BF₄⁻ in CH₃CN recorded at 0.1 to 10 A g⁻¹.

Table 1. Summary of specific capacitances in F g⁻¹ recorded by cyclic voltammetry.

| Scan rate mV s ⁻¹ | 1 | 2 | 5 | 10 | 20 | 50 | 100 | 200 |
|--|-----|-----|-----|-----|-----|----|-----|-----|
| 6M KOH in H ₂ O | | | | | | | | |
| BSA | 82 | 111 | 105 | 98 | 85 | 65 | 48 | 34 |
| GSA | 99 | 99 | 96 | 92 | 88 | 78 | 65 | 46 |
| MSA | 81 | 121 | 115 | 112 | 104 | 85 | 66 | 43 |
| PSA | 146 | 147 | 141 | 131 | 116 | 87 | 63 | 44 |
| 1M (C ₂ H ₅) ₄ N ⁺ BF ₄ ⁻ in CH ₃ CN | | | | | | | | |
| BSA | 102 | 100 | 94 | 89 | 81 | 68 | 57 | 46 |
| GSA | 96 | 94 | 89 | 84 | 77 | 63 | 50 | 37 |
| MSA | 93 | 90 | 84 | 78 | 71 | 60 | 50 | 39 |
| PSA | 83 | 81 | 77 | 73 | 68 | 60 | 53 | 44 |

Fig. 7d) and Table 3 show the capacitance vs. current density plots obtained in the galvanostatic charge/discharge experiments. At the lowest load of 0.1 A g⁻¹ specific capacitances range from 76 (PSA) to 98 (BSA) F g⁻¹. At the highest load of 10 A g⁻¹ there is still important capacitance of

ca. 20 to 25 F g⁻¹ in the materials with PSA being the leader. The voltage response vs. charging and discharging time for all current rates were placed in Fig. 9. For all samples the relationships were presented by typical triangular waveform with low IR drop.

Table 2. Summary of specific capacitances in F g⁻¹ recorded by electrochemical impedance.

| Frequency Hz | 0.001 | 0.01 | 0.1 | 1.0 | 10 | 100 | 1000 |
|--|-------|------|-----|-----|----|-----|------|
| 6M KOH in H ₂ O | | | | | | | |
| BSA | 117 | 106 | 73 | 42 | 14 | 2.3 | 0.20 |
| GSA | 104 | 97 | 86 | 63 | 29 | 3.4 | 0.14 |
| MSA | 123 | 116 | 93 | 52 | 12 | 2.7 | 0.28 |
| PSA | 161 | 147 | 97 | 43 | 24 | 5.3 | 0.21 |
| 1M (C ₂ H ₅) ₄ N ⁺ BF ₄ ⁻ in CH ₃ CN | | | | | | | |
| BSA | 97 | 85 | 67 | 31 | 10 | 2.0 | 0.24 |
| GSA | 92 | 76 | 51 | 26 | 9 | 1.5 | 0.09 |
| MSA | 90 | 75 | 57 | 28 | 11 | 2.0 | 0.12 |
| PSA | 80 | 68 | 53 | 27 | 12 | 3.0 | 0.18 |

Table 3. Summary of specific capacitances in F g⁻¹ recorded by galvanostatic charging-discharging.

| Current density A g ⁻¹ | 0.1 | 0.2 | 0.5 | 1.0 | 2.0 | 5.0 | 10.0 |
|--|-----|-----|-----|-----|-----|-----|------|
| 6M KOH in H ₂ O | | | | | | | |
| BSA | 113 | 108 | 97 | 82 | 64 | 41 | 17 |
| GSA | 101 | 100 | 97 | 93 | 84 | 68 | 45 |
| MSA | 121 | 117 | 108 | 101 | 89 | 62 | 27 |
| PSA | 143 | 140 | 130 | 115 | 88 | 54 | 36 |
| 1M (C ₂ H ₅) ₄ N ⁺ BF ₄ ⁻ in CH ₃ CN | | | | | | | |
| BSA | 98 | 92 | 81 | 71 | 58 | 42 | 29 |
| GSA | 90 | 86 | 78 | 67 | 54 | 38 | 26 |
| MSA | 87 | 81 | 72 | 63 | 54 | 38 | 27 |
| PSA | 76 | 73 | 67 | 61 | 54 | 42 | 34 |

A number of factors contribute to the final outcome of a carbonaceous material in terms of its specific capacitance in a symmetrical electrochemical double layer capacitor. Many authors have been trying to correlate a material's capacitance to its structure and physicochemical properties. As far as materials from biological residues only are considered, Sun et al. have very recently found that doping an activated carbon from rapeseeds with nitrogen can be a highly effective method for increasing the supercapacitor's capacitance in 6M KOH electrolyte, achieving a maximum capacitance of 250 F g⁻¹ in three-electrode cells [33]. On the other hand, strictly morphological features have also been highlighted as important factor determining the material's capacitance, with preference being given to nanorod and nanosheet morphologies [34] or to three-dimensional structures [35]. Many authors stress

the importance of the activation process, with special attention to the resultant porous structure, often with the application of a special porosity creating agent (some recent examples are based on the application of ZnCl_2 as the pore-forming agent [21,33,36] and phosphoric acid [37]. Subramanian et al. [21] pointed out on the basis of their study of banana fibers based carbon materials that surface area developed as the result of proper activation procedure played the crucial role in elevating the observed capacitances up to 30 times as compared to a untreated material. The role of the surface area development in the case of carbons derived from biomass waste has recently been extensively discussed by Jain et al. [38]. These findings are generally in agreement with the present work, however the importance of surface chemistry and surface acidity has relatively seldom been emphasized in recent reports [39,40]. Pandolfo et al. [5] pointed out that acidic surface groups, formed preferentially upon exposure to oxygen in temperatures between 200 °C and 700 °C, could be regarded as generally less stable than acidic and neutral groups which are formed at lower temperatures. Surface acidity can also exert strong influence on the self-discharge properties, with materials with a large concentration of surface carboxylic, lactonic and phenolic functionalities exhibiting generally higher leakage currents due to inherent instability.

Specific surface area is generally considered to be positively correlated with capacitance, however this is further co-determined by the porous structure, in particular how much of specific surface area is connected with micropores. Even more precisely: each particular electrolyte should favor a particular pore structure. This is because electrolyte species have to penetrate the pores so as to approach their inner walls. This is particularly striking when comparing aqueous media with organic ones. When inspecting the behavior of the four examined carbons it is evident that some of them perform in a dramatically different way in each of the two electrolytes. PSA is an excellent exemplification in that it has the highest capacitance (at least at low rates) in KOH and the lowest in the organic medium. For the purpose of purely utilitarian evaluation it is satisfactory enough to conclude that PSA is well suited for EDLCs with KOH based electrolytes.

Another interesting finding is that a carbon may perform poorly at low rates while being the best at higher rates, and vice versa. This is the case when comparing PSA and GSA in KOH based electrolyte. One can assume that PSA has a much more favorable porous structure for this aqueous medium than GSA, however the latter is characterized by better charge propagation and faster charge mobility at higher charge/discharge rates, which in fact makes this material overall more useful. Thus electronic conductivity is another factor to take into account [41-43]. Conductivity in turn may be affected by the degree of graphitization, grain size, basal to edge planes ratio and, last but not least, the procedure of electrode manufacturing. The last mentioned factor can, however, be assumed as equal for all the samples.

The process of activation creates new functional groups on the carbon surfaces. Nature of these surface chemistry is very difficult to determine but obviously it varies from one material to another due to the crucial role of the starting material chemistry. It is well known that surface chemistry brings about the phenomenon of pseudocapacitance, which is an additional capacitance due to faradaic reactions involving these functional groups. The exact impact of pseudocapacitance is beyond the scope of this work, but obviously affects the final result.

Having all this in mind, it can be summarized that materials obtained from waste fruit skins have demonstrated very high capacitances in EDLCs, making them a potentially promising energy materials of biological origin. All four materials exceeded 100 F g^{-1} in the aqueous medium and approached this value in the organic medium. Although PSA exhibits the highest capacitance at low rates in KOH, GSA should be identified as the most attractive material due to the fact that it preserves the capacitance at high rates. In the organic electrolyte all four materials behave similarly but GSA has a visible advantage and therefore might be recommended.

4. CONCLUSIONS

It has been successfully demonstrated that carbon materials obtained from food processing residues can be further utilized as fully viable electrode materials for electrochemical capacitors. The raw materials underwent thermal treatment with an innovative activation procedure to obtain materials with desirable morphology and structure. The whole procedure is environmentally friendly since it avoids more harmful activation agents such as KOH. The materials are characterized by high values of specific surface areas, close to those known for commercially available activated carbons. Also the capacitances determined with the application of several techniques have been found to approach state-of-the-art commercial carbons, ranging from 100 to 140 F g^{-1} in aqueous electrolyte and 80 to 120 F g^{-1} in organic electrolyte. More in-depth analysis of the materials detailed structural features and their correlation to the electrochemical performance will be subject to future work.

ACKNOWLEDGEMENTS

This work was supported by the Polish Ministry of Higher Education and Science (Project Iuventus Plus No. IP2012 004072)

This work was financially supported by Ministry of Science and Higher Education - statutory activity, decision number: 3787/E-138/S/2016

References

1. A.F. Burke, *J. Power Sources* 91 (2000) 37.
2. J.R. Miller, A.F. Burke, *Electrochem Society Interface* 17 (2008) 53.
3. E. Frąckowiak, F. Béguin, *Carbon* 39 (2001) 937.
4. F. Béguin, E. Frąckowiak, *Supercapacitors (New materials for sustainable energy and development)*. Wiley VCH Verlag GmbH, (2013).
5. A.G. Pandolfo, A.F. Hollenkamp, *J. Power Sources* 157 (2006) 11.
6. L.L. Zhang, X.S. Zhao, *Chem. Soc. Rev.* 38 (2009) 2520.
7. P. Simon, Y. Gogotsi, *Phil. Trans. R. Soc. A* 368 (2010) 3457.
8. G. Lota, T.A. Centeno, E. Frąckowiak, F. Stoeckli, *Electrochim Acta* 53 (2008) 2210.
9. P. Simon, Y. Gogotsi, *Acc. Chem. Res.* 46 (2013) 1094.
10. F. Béguin, V. Presser, A. Balducci, E. Frąckowiak, *Adv Mater.* 26 (2014) 2219.
11. C. Zhao, W. Zheng, *Front. Energy Res.* 3 (2015) 23.
12. P. McKendry, *Bioresour. Technol.* 83 (2002) 37.
13. K.G. Roberts, B.A. Gloy, S. Joseph, N.R. Scott, J. Lehmann, *Sci. Technol.* 44 (2010) 827.

14. C.E. Wyman, *Biotechnol. Prog.* 19 (2003) 254.
15. P. Nowicki, P. Skibiszewska, R. Pietrzak, *Adsorption* 19 (2013) 521.
16. K. Jurewicz, R. Pietrzak, P. Nowicki, H. Wachowska, *Electrochim Acta* 53 (2008) 5469.
17. J. Hayashi, A. Kazehaya, K. Muroyama, A.P. Watkinson, *Carbon* 38 (2000) 1873.
18. T.E. Rufford, D.H. Jurcakova, Z. Zhu, G.Q. Lu, *Electrochem Comm.* 10 (2008) 1594.
19. T.E. Rufford, D.H. Jurcakova, E. Fiset, Z. Zhu, G.Q. Lu, *Electrochem Comm.* 11 (2009) 974.
20. Lv, Y., Gan, L., Liu, M., Xiong, W., Xu, Z., Zhu, D., Wright, D.S., *J. Power Sources* 209 (2012) 152.
21. V. Subramanian, C. Luo, A.M. Stephan, K.S. Nahm, S. Thomas, B. Wei, *J. Phys. Chem. C* 111 (2007) 7527.
22. C. Penga, X. Yana, R. Wanga, J. Langa, Y. Ou, Q. Xue, *Electrochim Acta* 87 (2013) 401.
23. K. Wang, N. Zhao, S. Lei, R. Yan, X. Tian, J. Wang, Y. Song, D. Xu, Q. Guo, L. Liu, *Electrochim Acta* 166 (2015) 1.
24. X. Li, W. Xing, S. Zhuo, J. Zhou, F. Li, S.Z. Qiao, G.Q. Lu, *Bioresour. Technol.* 102 (2011) 1118.
25. A.E. Ismanto, S. Wang, F.E. Soetaredjo, S. Ismadji, *Bioresour. Technol.* 101 (2010) 3534.
26. R. Farma, M. Deraman, A. Awitdrus, I.A. Talib, E. Taer, N.H. Basri, J.G. Manjunatha, M.M. Ishak, B.N.M. Dollah, S.A. Hashmi, *Bioresour. Technol.* 132 (2013) 254.
27. M. Olivares-Marin, J.A. Fernandez, M.J. Lazaro, C. Fernandez-Gonzalez, A. Macias-Garcia, V. Gomez-Serrano, F. Stoeckli, T.A. Centeno, *Mater. Chem. Phys.* 114 (2009) 323.
28. H.P. Boehm, *Carbon* 32 (1994) 759.
29. P. Nowicki, H. Wachowska, R. Pietrzak, *J Hazard Mater.* 181 (2010) 1088.
30. K. Wasiński, M. Walkowiak, G. Lota, *J. Power Sources* 255 (2014) 230.
31. M.D. Stoller, R.S. Ruoff, *Energy Environ. Sci.* 3 (2010) 1294.
32. A. Burke, *Electrochim Acta* 53 (2007) 1083.
33. K. Sun, D. Guo, X. Zheng, Y. Zhu, Y. Zheng, M. Ma, G. Zhao, G. Ma, *Int. J. Electrochem. Sci.* 11 (2016) 4743
34. K. Sun, H. Wang, H. Peng, Y. Wu, G. Ma, Z. Lei, *Int. J. Electrochem. Sci.* 10 (2015) 2000
35. X. Chen, K. Wu, B. Gao, Q. Xiao, J. Kong, Q. Xiong, X. Peng, X. Zhang, J. Fu, *Waste Biomass Valor.* 7 (2016) 551
36. M.R. Jisha, Y.J. Hwang, J.S. Shin, K.S. Nahm, T.P. Kumar, K. Karthikeyan, N. Dhanikaivelu, D. Kalpana, N.G. Renganathan, A.M. Stephan, *Mater. Chem. Phys.* 115 (2009) 33
37. C.-K. Sim, S.R. Majid, N.Z. Mahmood, *Int. J. Electrochem. Sci.* 10 (2015) 10157
38. A. Jain, R. Balasubramanian, M.P. Srinivasan, *Chem. Eng. J.* 283 (2016) 789
39. J.M.V. Nabais, P. Nunes, P.J.M. Carrott, M.M.L. Ribeiro Carrott, A.M. García, M.A. Díaz-Díez, *Fuel Process Technol.* 89 (2008) 262
40. J.L. Figueiredo, M.F.R. Pereira, M.M.A. Freitas, J.J.M. Orfao, *Carbon* 37 (2009) 1379
41. M. Inagaki, H. Konno, O. Tanaike, *J. Power Sources* 195 (2010) 7880
42. J.A. Fernández, M. Arulepp, J. Leis, F. Stoeckli, T.A. Centeno, *Electrochim Acta* 53 (2008) 7111.
43. T.A. Centeno, M. Hahn, J.A. Fernández, R. Kötz, F. Stoeckli, *Electrochem Comm.* 9 (2007) 1242.